Phytochemistry 153 (2018) 36–47

Contents lists available at ScienceDirect

Phytochemistry

journal homepage: www.elsevier.com/locate/phytochem

Anti-inflammatory lignans and phenylethanoid glycosides from the root of *Isodon ternifolius* (D.Don) Kudô

Yanjun Zhang[a,b], Ke Wang[a], Huangcan Chen[a], Ruijie He[a], Runlin Cai[c], Jian Li[d], Dexiong Zhou[a], Wei Liu[a], Xishan Huang[c], Ruiyun Yang[a], Shengping Deng[a], Jun Li[a,*], Xinlan Guan[d,**]

[a] State Key Laboratory for the Chemistry and Molecular Engineering of Medicinal Resources, School of Chemistry and Pharmaceutical Sciences of Guangxi Normal University, Guilin, 541004, China
[b] School of Petroleum and Chemical Engineering, Qinzhou University, Qinzhou, 535000, China
[c] School of Chemistry, SunYat-sen University, Guangzhou, 510275, China
[d] Peoples' Hospital of Pubei, Pubei, 535300, China

ARTICLE INFO

Keywords:
Isodon ternifolius (D.Don) Kudô (Lamiaceae)
Lignans
Phenylethanoid glycoside
Anti-inflammation
LPS-induced RAW264.7 macrophage cells

ABSTRACT

Five undescribed lignans, three undescribed phenylethanoid glycosides and eight known compounds were isolated from the root of *Isodon ternifolius* (D.Don) Kudô (Lamiaceae). The structures of all of the isolated constituents were characterized by physical data analyses including NMR, MS and ECD. The anti-inflammatory activities of the isolates were evaluated based on their ability to inhibit NO, PGE2 and TNF-α production in LPS-induced RAW 264.7 macrophage cells. Six phenyl-naphthalene lignans, ternifoliuslignan A, ternifoliuslignan B, ternifoliuslignan C, ternifoliuslignan D, ternifoliuslignan E and 3-carboxy-6,7-dihydroxy-1-(3′,4′-dihydroxyphenyl) -naphthalene, can substantially inhibit the release of NO with IC_{50} values in the range of 9.98–29.14 μM, which are better than the positive reference. These phenyl-naphthalene lignans could markedly decrease the secretions of PGE2 and TNF-α in LPS-induced RAW264.7 cells. Ternifoliuslignan C and ternifoliuslignan D decreased iNOS, COX-2 and NF-κB/p65 protein expression. A preliminary structure-activity relationship among the phenyl-naphthalene lignans for the anti-inflammatory activity was discussed.

1. Introduction

The genus *Isodon* consists of approximately 150 species that are mainly distributed in the tropical and subtropical regions of Asia (Delectis Florae reipublicae popularis sinicae agendae academiae sinicae edita). The genus is famous for having been the source of more than 1200 new diterpenoids with diverse skeletons (Liu et al., 2017; Zou et al., 2012). Some species have been used in traditional medicine, e.g., *Isodon japonica* (Burm.f.) H. Hara has been traditionally used to treat hepatitis, gastritis, mastitis, stomach-aches and arthralgia (Chi et al., 2016); *Isodon rubescens* (Hemsl.) H. Hara has been used in traditional Chinese medicine (TCM) for its various activities, including anti-inflammatory, antitumour, antimicrobial, immunological and antioxidant activities, as well as its hypotensive effects (Guo et al., 2010); and the roots and aerial parts of *Isodon ternifolius* (D.Don) Kudô have been used in TCM to treat diarrhoea, enteritis, acute icterohepatitis, and other types of inflammation (Wu and Li, 1977). *I. ternifolius* is also a major ingredient of a Chinese patent medicine “Fufang Sanye xiangchacai Pian”, which is used to treat chronic and acute hepatitis and hepatitis B (Liu et al., 2017).

The anti-inflammatory potential of *Isodon* has been previously reported (Shin et al., 2004a, b; Hong et al., 2007; Lee et al., 2007). In our first study, the ethyl acetate extract of *I. ternifolius* showed decreased secretions of NO in LPS-induced RAW264.7 cells. To inspire further use of this plant and identify new anti-inflammatory agents, further investigations were carried out. The structures of all isolated constituents were characterized by comprehensive spectroscopic analyses, and the absolute configurations were elucidated by quantum chemical CD calculations. These findings have led to the isolation of five undescribed lignans (**1–5**), three undescribed phenylethanoid glycosides (**6–8**), three known lignans (**9**−**11**), three phenylpropanoids (**12–14**) and two phenylethanol derivatives (**15–16**) (Fig. 1). The anti-inflammatory effects of all isolates were evaluated with regard to their activities on the production of NO and pro-inflammatory cytokines TNF-α and PGE2 in vitro by using LPS-activated RAW264.7 macrophage cells. Furthermore, the anti-inflammatory mechanisms of some compounds were clarified by western blot analysis. We also explored the structure−activity relationships among some lignans obtained from *I. ternifolius*. The

* Corresponding author.
** Corresponding author.
E-mail addresses: lijun9593@gxnu.edu.cn (J. Li), 717433739@qq.com (X. Guan).

https://doi.org/10.1016/j.phytochem.2018.05.017
Received 2 March 2018; Received in revised form 15 May 2018; Accepted 26 May 2018

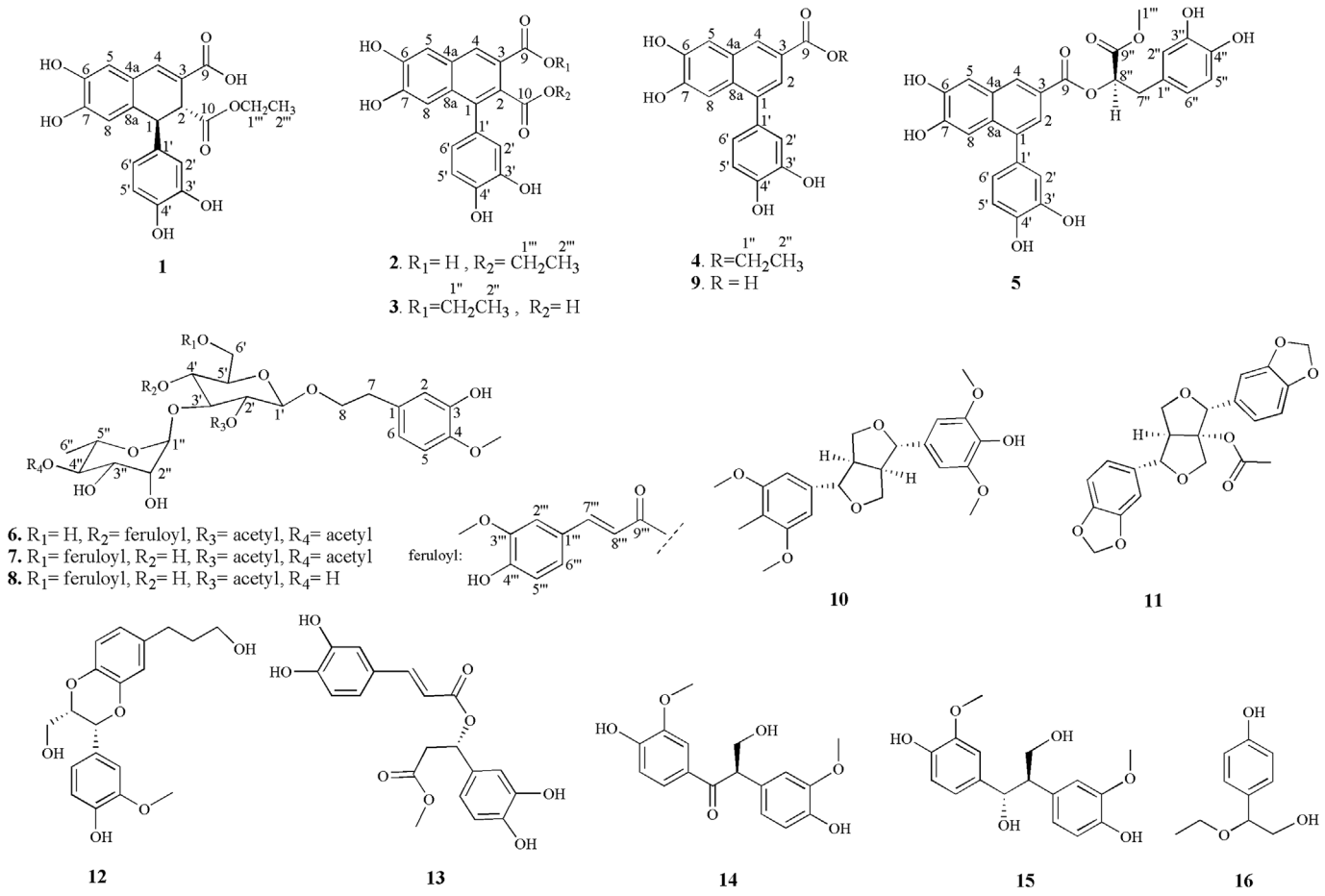

Fig. 1. Structures of compounds **1–16**.

research provided the basis for expanding the utilization and development of this medicinal plant.

2. Results and discussion

2.1. Structural elucidation of the new compounds

The molecular formula of ternifoliuslignan A (**1**) was determined as $C_{20}H_{18}O_8$ based on the sodium adduct ion at *m/z* 409.0896 $[M + Na]^+$ (calcd for $C_{20}H_{18}O_8Na$ 409.0899) in its HRESIMS, which suggests 12 degrees of unsaturation. The ^1H NMR spectrum showed eight methine protons [δ_H 4.34 (d, J = 4.3 Hz), 3.84 (d, J = 4.3 Hz); 6.47 (d, J = 2.1 Hz), 6.65 (d, J = 8.1 Hz) and 6.40 (dd, J = 8.1, 2.1 Hz) attributed to a 1,2,4-trisubstituted aromatic moiety and three singlets at δ_H 7.57, 6.82, and 6.50 (1H each)]; one oxygenated methylene proton at δ_H 4.04 (q, J = 7.1 Hz); and one methyl signal at δ_H 1.12 (t, J = 7.1 Hz). The coupling constant of the methyl signal (7.1 Hz) indicated the presence of an ethoxy group (Table 1). The ^{13}C NMR spectrum showed 20 signals comprising two carboxylic carbons (δ_C 170.7 and 175.0), fourteen aromatic or olefinic carbons, and four sp^3 carbons (two methine carbons, one methylene carbon and one methyl carbon attributed to an ethoxy group) (Table 2). These data are similar to those of a phenyldihydronaphthalene moiety (Chawla et al., 1992). In the HMBC experiment, the correlations from H-1 to C-2′, C-6′, C-8 and C-10; H-4 to C-2, C-5, C-8a and C-9; and H-1‴ to C-10 showed that the ethoxy group was linked to C-10 (Fig. 2). The relative configuration of **1** was inferred from coupling constant between H-1 and H-2 and a ROESY experiment. The coupling constant (J = 4.3 Hz) between H-1 and H-2 was in accordance with a relative 1,2-trans-configuration (Ma et al., 2007), moreover, the ROESY spectrum of compound **1** showed correlation between the signals at δ_H 4.34 (H-1) and δ_H 6.50 (H-8) as well as between the signals at δ_H 3.84 (H-2) and δ_H 6.47 (H-2′) (Fig. 3) which suggested a trans relative configuration between H-1 and H-2 (Fig. 3) (Ren et al., 2017). Furthermore, the absolute structure of **1** was confirmed by the ECD spectrum, which showed a positive Cotton effect at 209 and 373 nm and a negative Cotton effect at 240 and 343 nm. The experimental ECD spectrum of **1** coincided with the calculated ECD spectrum of (1*S*,2*R*)-**1** (Fig. 4), which are similar to those of compound **2b** [dimethyl (1*S*,2*R*)-1-(3,4-dimethoxyphenyl)-6,7-dimethoxy-1,2-dihydronaphthalene-2,3-dicarboxylate] (Nishizawa et al., 1990) and compound **4a** [dimethyl (1*S*,2*R*)-1-(3,4-dihydroxyphenyl)-6,7-dihydroxy −1,2-dihydronaphthalene-2,3-dicarboxylate] (Ren et al., 2017). Thus, compound **1** was identified as (1*S*,2*R*)-2,3-dicarboxy-6,7-dihydroxy-1-(3′,4′-dihydroxy)-phenyl-1,2-dihydro-naphthalene-10-ethyl ester and named ternifoliuslignan A.

Ternifoliuslignan B (**2**) was determined to have the formula $C_{20}H_{16}O_8$ based on the sodium adduct ion at *m/z* 383.0754 $[M - H]^-$ (calcd for $C_{20}H_{15}O_8$ 383.0767) in its HRESIMS, which indicates 13 degrees of unsaturation. Compared to compound **1**, compound **2** is missing two protons and has one additional degree of unsaturation, which suggested the presence of a C-1/C-2 double bond. This feature was confirmed by the NMR spectra (Table 2). The ^{13}C NMR signal of C-1 shifted from δ_C 47.3 in **1** to δ_C 137.8 in **2**, and C-2 shifted from δ_C 49.4 in **1** to δ_C 129.8 in **2**. In the HMBC spectrum, the correlation from H-1‴ to C-10 showed that the ethoxy group was linked to C-10. Meanwhile, the correlations from H-6′ to C-1, C-2′, and C-4′ as well as the correlations from H-2′ to C-1, C-4′ and C-6′ showed that the 3′,4′-dihydroxyphenyl moiety was linked to the naphthalene (Fig. 5). Thus, the structure of **2** was established to be 2,3-dicarboxy-6,7-dihydroxy-1-(3′,4′-dihydroxy)-phenylnaphthalene-10-ethyl ester and named

Table 1
^{1}H NMR data (400 MHz, CD_3OD) for ternifoliuslignans A − E (**1–5**).

Position	ternifoliuslignan A (1)	ternifoliuslignan B (2)	ternifoliuslignan C (3)	ternifoliuslignan D (4)	ternifoliuslignan E (5)
	δ_H (*J* in Hz)	δ_H (*J* in Hz)	δ_H (*J* in Hz)	δ_H (*J* in Hz)	δ_H (*J* in Hz)
1	4.34, d (4.3)				
2	3.84, d (4.3)			7.65, d (1.4)	7.63, d (1.5)
3					
4	7.57, s	8.31, s	8.26, s	8.26, d (1.4)	8.25, d (1.5)
4a					
5	6.82, s	7.27, s	7.26, s	7.28, s	7.28, s
6					
7					
8	6.50, s	6.94, s	6.91, s	7.30, s	7.30, s
8a					
9					
10					
1′					
2′	6.47, d (2.1)	6.75, d (2.0)	6.78, d (2.0)	6.91,d (2.1)	6.90, d (2.1)
3′					
4′					
5′	6.65, d (8.1)	6.86, d (8.0)	6.85, d (8.0)	6.92, d (8.0)	6.92, d (8.0)
6′	6.40, dd (8.1, 2.1)	6.61, dd (8.0, 2.0)	6.65, dd (8.0, 2.0)	6.79, dd (8.0, 2.1)	6.78, dd (8.0, 2.1)
1″			4.36, q (7.1)	4.36, q (7.1)	
2″			1.40, t (7.1)	1.40, t (7.1)	6.77, d (2.0)
3″					
4″					6.71, d (8.1)
5″					6.64, dd (8.1, 2.0)
6″					
7″					3.17, dd (12.5, 7.2)
					3.12, dd (12.5, 5.5)
8″					5.35, dd (7.2, 5.5)
9″					
1‴	4.04, q (7.1)	4.05, q (7.1)			3.73, s
2‴	1.12, t (7.1)	1.07, t (7.1)			

Table 2
^{13}C NMR data (100 MHz, CD_3OD) for ternifoliuslignans A − E (**1–5**).

Position	ternifoliuslignan A (1)	ternifoliuslignan B (2)	ternifoliuslignan C (3)	ternifoliuslignan D (4)	ternifoliuslignan E (5)
	δ_C, type	δ_C, type	δ_C, type	δ_C, type	δ_C, type
1	47.3, CH	137.8, C	137.3, C	140.1, C	140.2, C
2	49.4, CH	129.8, C	129.6, C	124.2, C	124.6, CH
3	123.8, C	123.5, C	123.2, C	125.5, C	124.3, C
4	139.5, CH	130.2, CH	129.8, CH	129.0, CH	129.5, CH
4a	131.3	130.3, C	131.2, C	130.4, C	130.3, C
5	117.0, CH	111.8, CH	111.8, CH	112.2, CH	112.4, CH
6	145.5, C	149.1, C	149.1, C	148.3, C	148.3, C
7	148.9, C	150.5, C	150.6, C	150.1, C	150.3, C
8	117.0, CH	110.2, CH	110.3, CH	109.4, CH	109.4, CH
8a	125.1, C	132.0, C	132.2, C	131.8, C	132.0, C
9	170.7, C	169.5, C	168.2, C	169.0, C	168.2, C
10	175.0, C	172.2, C	174.5, C		
1′	135.8, C	130.1, C	130.5, C	133.9, C	133.7, C
2′	116.0, CH	118.7, CH	118.8, CH	118.0, CH	118.0, CH
3′	146.0, C	145.9, C	145.9, C	146.2, C	146.2, C
4′	145.0, C	146.1, C	146.1, C	145.9, C	145.9, C
5′	116.2, CH	115.9, CH	116.0, CH	116.3, CH	116.4, CH
6′	120.2, CH	123.1, CH	123.2, CH	122.3, CH	122.4, CH
1″			62.4, CH_2	62.0, CH_2	128.8, C
2″			14.4, CH_3	14.7, CH_3	117.6, CH
3″					146.2, C
4″					145.4, C
5″					116.4, CH
6″					122.0, CH
7″					38.0, CH_2
8″					75.1, CH
9″					172.2, C
1‴	62.1, CH_2	62.2, CH_2			52.8, CH_3
2‴	14.3, CH_3	14.0, CH_3			

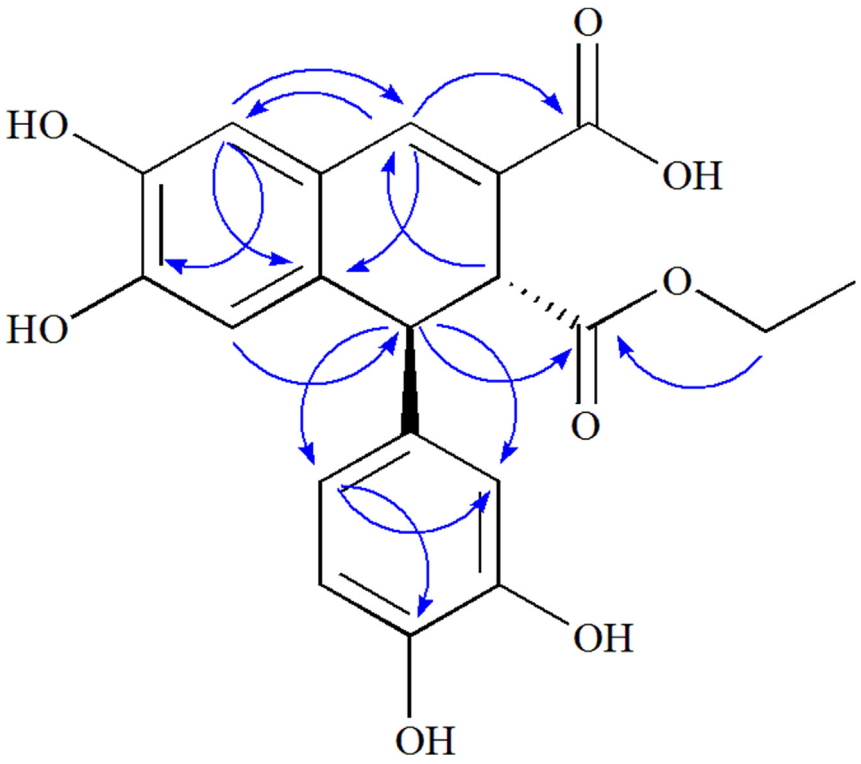

Fig. 2. Selected HMBC (arrows) correlations of **1**.

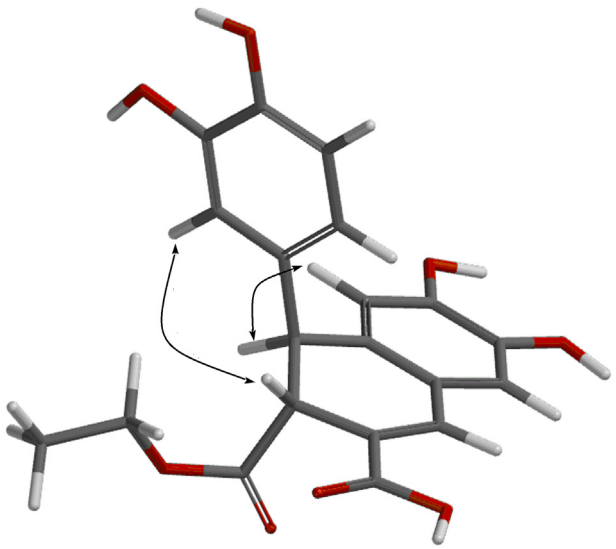

Fig. 3. ROESY correlations of **1**.

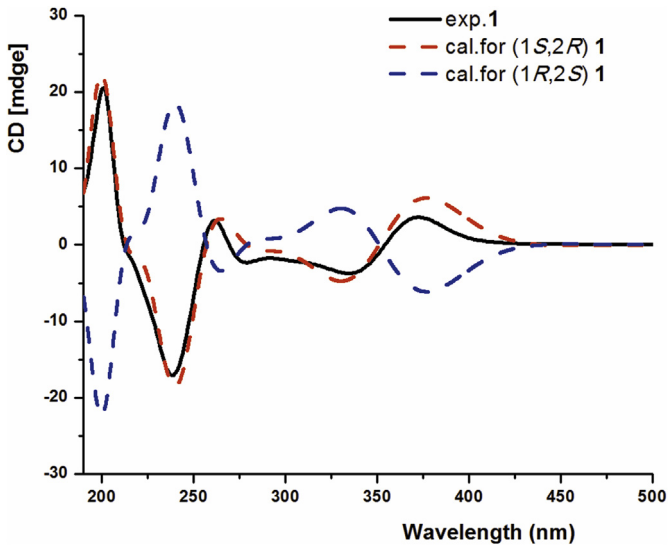

Fig. 4. Experimental and calculated ECD spectra of **1**.

ternifoliuslignan B.

Ternifoliuslignan C (**3**) has the same molecular formula ($C_{20}H_{16}O_8$) as **2** based on the HRESIMS data. The NMR data of **3** were similar to those of **2** (Tables 1 and 2); the differences in the ^{13}C NMR chemical shifts [− 1.3 ppm (C-9) and +2.3 ppm (C-10)] and the ^{1}H NMR chemical shifts [+ 0.33 ppm (−CH_2−) and +0.31 ppm (−CH_3), ethyl proton signals] indicated that the ethoxy group was linked to a different carboxyl group in **3** than it was in **2**. In the HMBC spectrum of **3** (Fig. 5), the correlations from H-4 to C-2, C-5, C-8a, and C-9 as well as from H-1″ to C-9 suggested that the ethoxy group was linked to C-9 in **3**. Thus, the structure of **3**, ternifoliuslignan C, was established to be 2,3-dicarboxy-6,7-dihydroxy-1-(3′,4′-dihydroxy)-phenyl-naphthalene-9-ethyl ester.

Ternifoliuslignan D (**4**) gave an $[M + Na]^+$ peak at *m/z* 363.0857 in its HRESIMS spectrum, which indicated a molecular formula of $C_{19}H_{16}O_6$. The NMR data of **4** (Tables 1 and 2) were similar to those of **3** except for the absence of the signals from the C-2 carboxyl group, indicating the quaternary C-2 carbon in **3** was a methine carbon in **4**. The coupling constant between H-2 and H-4 of 1.4 Hz indicated that the two protons were meta to each other in **4**. This conclusion was confirmed by the HMBC correlations (Fig. 5) of H-2 with C-1′, C-4 and C-9 (the ester carbonyl carbon), as well as the correlations of H-4 with C-2, C-5, C-8a, and C-9. Based on a comparison of the NMR data of **4** and **9**, a C_2H_5 unit is present in **4** that was not present in **9**, which indicates that the carboxyl group was ethyl esterified. The structure of 4 was determined to be 3-carboxy-6,7-dihydroxy-l-(3′,4′- dihydroxy)-phenylnaphthalene-9-ethyl ester and named ternifoliuslignan D.

Ternifoliuslignan E (**5**) gave an $[M - H]^-$ peak at *m/z* 505.1118

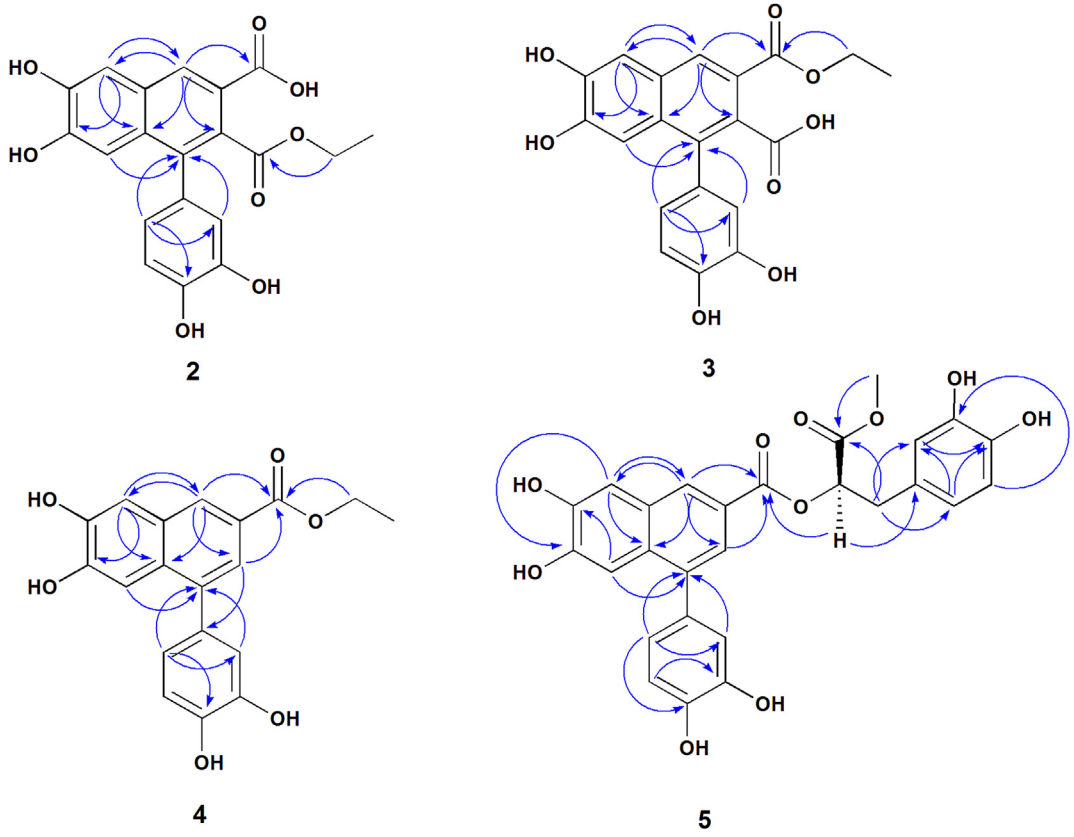

Fig. 5. HMBC correlations of **2–5**.

(calcd for $C_{27}H_{21}O_{10}$ 505.1135) in its HRESIMS spectrum, which indicated a molecular formula of $C_{27}H_{22}O_{10}$. Analysis of the ^{1}H and ^{13}C NMR data along with the aid of HSQC and DEPT experiments revealed that **5** had similar signals to those of eritrichin (Fedroreyev et al., 2005), and it differed only by the presence of a methoxy group instead of a hydroxy group at the 9″ position. The remaining signals included those of one methoxy proton at δ_H 3.73 (3H, s) corresponding to a carbon at δ_C 52.8, which indicated that the carboxyl group was methyl esterified. This conclusion was confirmed by the HMBC correlations of the methoxyl protons (H-1‴) to the carbonyl carbon (C-9″) (Fig. 5).

The absolute configuration of **5** was determined by comparing its optical rotation and CD data to those of eritrichin. Compound **5** showed an optical rotation of $[\alpha]_D^{25}$ + 35.0, a positive Cotton effect at 210 and 250 nm, and a negative Cotton effect at 228 nm in the CD curve, which were the same as those of eritrichin, suggesting that **5** has the same absolute configuration as that of eritrichin (see supporting information, Fig. S30). Therefore, the structure of **5**, ternifoliuslignan H, was established to be 2R-3-(3,4-dihydroxy-phenyl)-2-[(3,4-dihdroxyphenyl) −6,7-dihydroxy-2-naphthoyl-oxy]-propanoic acid methyl ester.

Ternifoliusoside F (**6**) was isolated as a yellow gum with an optical rotation of $[\alpha]_D^{25}$ − 15.7 (*c* 0.20, MeOH). The phenylethanoid glycoside HRESIMS data of *m/z* 759.2472 ([M + Na] $^{+}$, calcd for $C_{35}H_{44}O_{17}Na$, 759.2476) collected in the positive ion mode suggested a molecular formula of $C_{35}H_{44}O_{17}$ with 14 degrees of unsaturation. The ^{1}H NMR spectrum of **6** showed signals assignable to three methyl groups at δ_H 1.98 (3H, s), 1.76 (3H, s), and 0.99 (3H, d, J = 6.2 Hz); six methines attributed to two 1,2,4-trisubstituted aromatic moieties at δ_H 6.62 (dd, J = 8.2, 1.2 Hz), 6.81 (d, J = 8.2 Hz), 6.69 (d, J = 1.2 Hz), 7.08 (dd, J = 8.0, 1.2 Hz), 6.81 (d, J = 8.0 Hz), and 7.19 (d, J = 1.2 Hz); and two trans olefinic protons at δ_H 6.35 (1H, d, J = 15.9 Hz) and 7.65 (1H, d, J = 15.9 Hz) (Table 3). The ^{13}C NMR, DEPT and HSQC spectra displayed 35 carbon resonances that were identified as nine non-protonated carbons (three ester carbonyl carbons and six olefinic carbons); eighteen methine carbons (eight olefinic carbons and ten sp^3 oxygen-bearing carbons); three sp^3 methylene carbons, including two oxygen bearing carbons; and five methyl carbons, including two methoxyl carbons. Considering the three carbonyl carbons, two sets of aromatic ring carbons and a pair of olefinic carbons, two degrees of hydrogen deficiency remain, indicating the presence of two rings. The ^{13}C NMR and HSQC spectra showed two anomeric carbon to proton couplings (δ_C 101.6 with δ_H 4.53 and δ_C 102.2 with δ_H 4.85), which indicated the presence of two glycones. The proton signal at δ_H 1.00 (3H, d, J = 6.2 Hz) indicated the existence of a rhamnose group. The coupling between δ_H 3.34 (1H, m) and 3.57 (1H, m) with δ_C 62.1 in the HSQC indicated the presence of a glucose group. The $^{1}H-^{1}H$ COSY cross-peaks of H-1′/H-2′/H-3′/H-4′/H-5′ and H-1″/H-2″/H-3″/H-4″/H-5″/H-6″ confirmed the presence of two glycones (Fig. 6). The HMBC correlations from the methoxy group at δ_H 3.87 (s, 3H) to C-3‴, from H-5‴ to C-1‴ and C-3‴, and from H-7‴ to C-2‴, C-6‴ and C-9‴, suggested the presence of a feruloyl moiety. The correlations from the two proton signals of H-6′ at δ_H 3.34 and 3.57 with C-4′ and C-5′, and from H-4′ to C-9‴ showed that the feruloyl moiety might be linked at C-4′ (Glc-C-4). The HMBC cross-peak from H-3′ (Glc-H-3) to C-1″ (Rha-C-1) indicated that the rhamnopyranosyl moiety was linked at C-3′ (Glc-C-3). The HMBC correlations from the protons of the methoxy group at δ_H 3.81 (3H, s) to C-4, from H-6 to C-2 and C-4, from H-1′ to C-8, and from H-8 to C-1 and C-1′ showed that the phenylethanol moiety was linked to C-1′ (Glc-C-1). The HMBC correlations of the two methyl signals at δ_H 1.98 and 1.76 with carbonyl carbons (δ_H 1.98 with 171.3 and δ_H 1.76 with 172.4), H-2′ (Glu-H-2) with C-1′ and 171.3, H-4″ (Rha-H-4) with 172.4, and δ_H 0.99 (Rha-H-6) with C-4″ suggested the positions of the two acetyl groups. The relative configuration of the anomeric carbon of the Glc residue was determined to be β from the coupling constant (J = 8.0 Hz) of the anomeric proton. In the case of the Rha residue, the configuration of the anomeric proton was determined by comparison of the NMR data of compound **3** with those reported in the literature (Liu

Table 3
NMR data (400 MHz, CD_3OD) for ternifoliusosides F—H (**6–8**).

Position	ternifoliusoside F (**6**)		ternifoliusoside G (**7**)		ternifoliusoside H (**8**)	
	δ_C, type	δ_H (*J* in Hz)	δ_C, type	δ_H (*J* in Hz)	δ_C, type	δ_H (*J* in Hz)
1	133.2 C		133.0 C		133.0, C	
2	117.1, CH	6.69, d (1.2)	117.0, CH	6.66, d (2.0)	117.0, CH	6.69, d (1.5)
3	147.2, C		147.2, C		147.2, C	
4	147.4, C		147.4, C		147.4, C	
5	112.8, CH	6.81, d (8.0)	112.7, CH	6.70, d (8.0)	112.8, CH	6.71, d (8.0)
6	121.2, CH	6.62, dd (8.2, 1.2)	121.1, CH	6.58, dd (8.2, 2.0)	121.1, CH	6.62, dd (8.2, 1.5)
7	36.2, CH_2	2.72, m	36.4, CH_2	2.70, m	36.4, CH_2	2.72, m
8	71.6, CH_2	4.08, m; 3.64, m*	71.8, CH_2	3.96, m; 3.62, m*	71.7, CH_2	3.97, m; 3.67, m*
1′	101.6, CH	4.53, d (8.0)	101.8, CH	4.48, d (8.0)	101.8, CH	4.51, d (8.0)
2′	75.3, CH	4.87, m	75.0, CH	4.81, m	74.9, CH	4.81, m
3′	78.7, CH	4.03, m	82.1, CH	3.68, m*	82.6, CH	3.67, m*
4′	70.4, CH	5.01, m	70.5, CH	3.47, m*	70.5, CH	3.49, m*
5′	75.9, CH	3.59, m*	75.5, CH	3.59, m*	75.4, CH	3.75, m
6′	62.1, CH_2	3.34, m; 3.57, m*	64.4, CH_2	4.38, m; 4.50, m	64.4, CH_2	4.41, m; 4.54, m
1″	102.2, CH	4.85, br s	102.6, CH	4.84, br s	102.9, CH	4.82, br s
2″	72.4, CH	3.67, m*	72.4, CH	3.73, m*	72.5, CH	3.72, m*
3″	69.8, CH	3.61, m*	70.2, CH	3.79, m*	72.1, CH	3.64, m*
4″	75.1, C	4.77, m	75.4, CH	4.93, m	73.7, C	3.38, m*
5″	68.3, CH	3.68, m*	68.0, CH	4.16, m	70.3, CH	3.97, m
6″	18.1, CH_3	0.99, d (6.2)	17.6, CH_3	1.11, d (6.2)	17.8, CH_3	1.25, d (6.2)
1‴	127.4, C		127.7, C		127.5, C	
2‴	111.9, CH	7.19, d (1.2)	111.7, CH	7,16, d (1.8)	111.6, CH	7.18, d (1.2)
3‴	149.4, C		149.3, C		149.4, C	
4‴	151.0, C		150.6, C		150.9, C	
5‴	116.6, CH	6.81, d (8.0)	116.5, CH	6.81, d (8.0)	116.5, CH	6.81, d (8.0)
6‴	124.4, CH	7.08, d (8.2, 1.2)	124.3, CH	7.04, d (8.2, 1.8)	124.4, CH	7.06, d (8.2, 1.2)
7‴	148.1, CH	7.65, d (15.9)	147.2, CH	7.63, d (15.9)	147.2, CH	7.62, d (15.9)
8‴	114.7, CH	6.35, d (15.9)	115.2, CH	6.40, d (15.9)	115.1, CH	6.38, d (15.9)
9‴	167.9, C		169.0, C		169.1, C	
2′—O—$\underline{C}OCH_3$	171.3, C		171.6, C		171.6, C	
$COCH_3$	20.9, CH_3	1.98, s	21.0, CH_3	2.05, s	20.9, CH_3	1.98, s
4″—O—$\underline{C}OCH_3$	172.4, C		172.6, C			
$COCH_3$	20.7, CH_3	1.76, s	20.9, CH_3	1.99, s		
4-OCH_3	56.5, CH_3	3.81, s	56.4, CH_3	3.76, s	56.4, CH_3	3.76, s
3‴—OCH_3	56.5, CH_3	3.87, s	56.5, CH_3	3.86, s	56.4, CH_3	3.86, s

(*) indicate overlapped signals.

et al., 2014). In addition, acid hydrolysis of **6** liberated rhamnose (Rha) and glucose (Glc), and the relative configurations of the two hexoses were determined by TLC and HPLC analyses (see Experimental Section). Thus, the structure of compound **6** was determined to be 1′-*O*-*β*-D-(3-hydroxy-4-methoxy-phenyl)-ethyl-4′-*O*-feruloyl-*α*-L-(4″-acetyl)-rhamnosyl (1″→3′)-2′- acetyl-glucopyranoside, and it was named ternifoliusoside F.

Ternifoliusoside G (**7**) was obtained as a yellow gum with an optical rotation of $[\alpha]_D^{25}$ − 43.5 (*c* 0.20, MeOH). The HRESIMS data collected in the positive ion mode (*m/z*, 759.2469 [M + Na] $^+$, calcd for $C_{35}H_{44}O_{17}Na$, 759.2476) suggested a molecular formula of $C_{35}H_{44}O_{17}$, which is the same as that of ternifoliusoside F (**6**). Compound **7** exhibited similar NMR data to those of **6** (Table 3), suggesting that **7** has the same 2D structure as **6**. Compared to the spectral data of compound **6**, the downfield shifting of H-6′ from δ_H 3.34 and 3.57 to 4.38 and 4.50, and C-6 from δ_C 62.1 to 64.4, the up-field shifting of H-4′ from δ_H 5.01 to 3.47, and the correlation of H-6′ with the carbonyl carbon of the feruloyl moiety (C-9‴, δ_C 169.0) in the HMBC spectrum indicated that the feruloyl moiety was linked at C-6′ (Glc-C-6). The detailed HMBC correlations can be found in Fig. 6. Thus, the structure of **7** was established to be 1′-*O*-*β*-D-(3-hydroxy-4-methoxyphenyl)-ethyl-6′-*O*-feruloyl-*α*-L-(4″- acetyl)-rhamnosyl (1″→3′)-2′-acetyl-glucopyranoside and named ternifoliusoside G.

Ternifoliusoside H (**8**) was obtained as an amorphous powder with an optical rotation of $[\alpha]_D^{25}$ − 33.5 (*c* 0.21, MeOH). The HRESIMS data collected in the positive ion mode (*m/z*, 717.2365 [M + Na] $^+$, calcd for $C_{34}H_{42}O_{16}Na$, 717.2370) suggested a molecular formula of $C_{34}H_{42}O_{16}$, which is 42 mass units less than that of **7**. Comparison of the NMR data of **8** and **7** revealed that **8** was missing the signals from an acetyl group, which was consistent with the mass difference (Table 3). The differences in the ^{13}C NMR chemical shifts of **8** and **7** (−1.7 ppm (C-4″), +2.3 ppm (C-5″), and +1.9 ppm (C-3″)] indicated that the acetyl group at C-4″ of the rhamnose moiety in **7** had disappeared. Other than the 4″-acetyl signal, the other correlations in the HMBC spectrum of **8** were similar to those of **7** (Fig. 6). Thus, the structure of **8**, ternifoliusoside H, was established to be 1′-*O*-*β*-D-(3-hydroxy-4-methoxyphenyl)-ethyl-6′-*O*-feruloyl-*α*-L-rhamnosyl (1″→3′)-2′-acetyl-glucopyranoside.

The eight known compounds were identified by NMR and MS, as well as by comparison with the literature data as 3-carboxy-6,7-dihydroxy-1-(3′,4′-dihydroxy phenyl)-naphthalene (**9**) (Xie et al., 2007), (+)-syringaresinol (**10**) (Deyama et al., 1987), 1-acetoxyl-2e,6e-dipiperonyl-3,7-dioxabicyclo -[3,3,0]-octane (**11**) (Jiang et al., 2000), (7*S*,8*S*)-3-methoxy-3′,7-epoxy-8,4′-oxyneolignan-4,9,9′ -triol (**12**) (Xu et al., 2006), 3-(3,4-dihydroxyphenyl)-acrylic acid-1-(3,4-dihydroxyphenyl)-2- methoxy carbonyl ethyl ester (**13**) (Lee et al., 2001), oxyneolignan A (**14**) (Sun et al., 2015), evofolin-B (**15**) (Wu et al., 1995), and 1,2-*bis* (4-hydroxy-3-methoxyphenyl)-1,3-propanediol (**16**) (Yoshikawa et al., 1998).

2.2. Anti-inflammatory activity

2.2.1. Effects of all compounds on the production of NO in LPS-induced RAW 264.7 cells

The cell viability assay showed that the survival rates of RAW264.7 macrophages cells were over 90% for all compounds at all

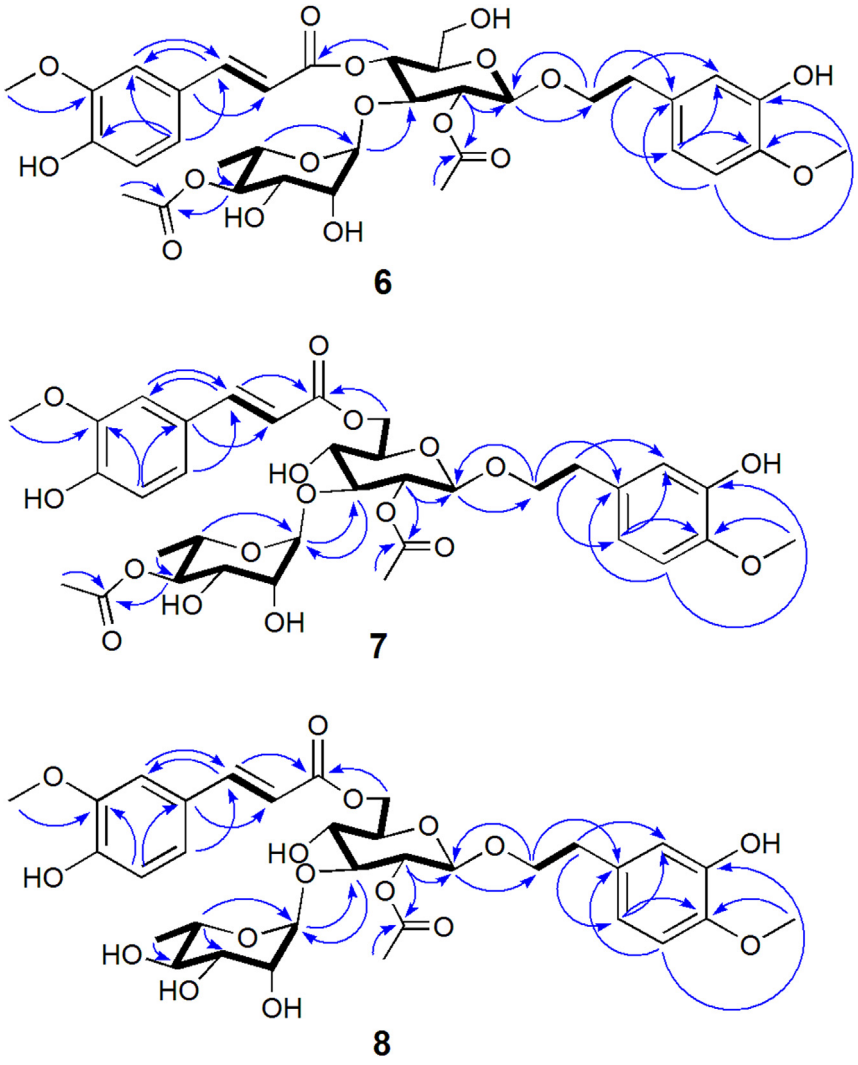

Fig. 6. Selected HMBC (arrows), $^{1}H-^{1}H$ COSY (bonds) correlations of **6–8**.

Table 4
Inhibitory activities on NO of all compounds in LPS-induced RAW 264.7 cell.[a].

Compound	IC_{50} (μM)
1	25.01 ± 0.29
2	23.90 ± 0.42
3	18.64 ± 0.15
4	9.98 ± 0.21
5	29.14 ± 0.14
6	> 50
7	> 50
8	> 50
9	24.54 ± 0.62
10	37.45 ± 0.43
11	38.59 ± 0.34
12	45.71 ± 0.21
13	35.43 ± 0.64
14	42.41 ± 0.73
15	> 50
16	> 50
Indomethacin[b]	35.39 ± 0.24

[a] All values are means of three independent experiments.

[b] Indomethacin, an anti-inflammatory agent, is used as positive control.

concentrations from 0 to 50 μM. Macrophages are the important immune cells in mammals and produce a great amount of NO after being stimulated by LPS, which results in inflammation (Wang et al., 2016). The anti-inflammatory activities of all isolates were evaluated in terms of their ability to inhibit NO production in LPS-induced RAW 264.7 cells. From the results in Table 4, it was concluded that the six phenyl-naphthalene lignans, compounds **1**, **2**, **3**, **4**, **5** and **9**, can substantially inhibit the release of NO with IC_{50} values in the range of 9.98–29.14 μM, which are better than the positive reference indomethacin. The nonphenyl-naphthalene lignans, compounds **10** and **11**, had moderate effects with IC_{50} values of 37.45 μM and 38.59 μM, respectively, which are slightly weaker than indomethacin. Compound **13** has an activity approximately equal to that of indomethacin, and the other compounds including phenylethanoid glycosides **6–8** and phenylethanol derivatives **15–16** displayed IC_{50} values greater than 50 μM. These results suggest the anti- inflammatory effects of the phenyl-naphthalene lignans.

2.2.2. Effects of the phenyl-naphthalene lignans on the production of TNF-α and PGE2 in LPS-induced RAW264.7 cells

To further investigate the anti-inflammatory activity of the phenyl-naphthalene lignans, TNF-α and PGE2, two crucial pro-inflammatory mediators, were measured in LPS-stimulated RAW264.7 cells after treatment with the phenyl-naphthalene lignans (Figs. 7 and 8). The production of TNF-α and PGE2 was significantly increased with LPS

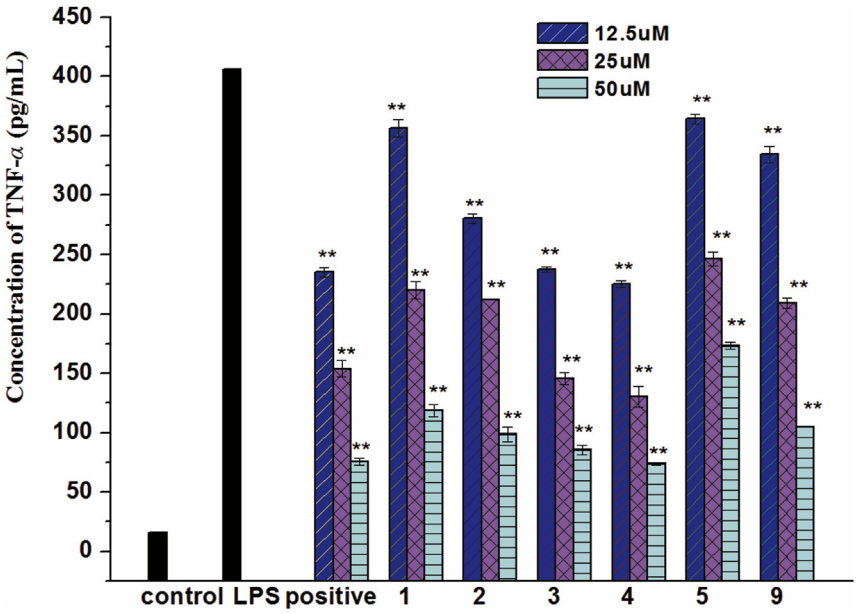

Fig. 7. Effects of the compounds **1**, **2**, **3**, **4**, **5** and **9** on the TNF-*α* production in LPS-stimulated RAW 264.7 cells. The cells were stimulated with LPS (100 ng/mL) 2 h and then for treated with the compounds (12.5, 25, 50 μM) for 24 h. TNF-*α* concentration in the supernatants was measured using ELISA. Indomethacin was used as positive reference compound at the same concentration with compounds. Values are the mean ± SE of three determinations. **p < 0.01, *p < 0.05 compared with cells treated by LPS.

stimulation. However, the over-production of TNF-*α* and PGE2 was considerably reduced by treatment with the phenyl-naphthalene lignans (compounds **1**, **2**, **3**, **4**, **5** and **9**). Generally, the data indicated that these compounds can suppress the LPS-induced production of inflammatory cytokines (TNF-*α* and PGE2) in a concentration-dependent manner in RAW 264.7 cells. Notably, at the same concentration, the inhibitory effects of compound **4** on the production of TNF-*α* and PGE2 were significant stronger than those of the other phenyl-naphthalene lignans and positive control reference indomethacin. The inhibitory effect of compound **3** was equivalent to that of indomethacin. The inhibitory effects of other phenyl-naphthalene lignans were weaker than that of the positive control drug. Furthermore, a comparison of the inhibitory effects of **1** and **2** as well as **9** and **5** at the same concentration on the production of TNF-*α* and PGE2 showed that the inhibitory effect of **2** is stronger than that of **1**, and the inhibitory effect of **9** is stronger than that of **5**.

*2.2.3. Effects of compounds **3** and **4** on iNOS, NF-κB/p65 and COX-2 protein expression in LPS-induced RAW 264.7 cells*

NF-*κ*B is one of the pivotal transcription factors that controls the expression of inflammatory enzymes and inflammatory mediators. Moreover, iNOS and COX-2 are two important pro-inflammatory mediators during the inflammatory process (Yeom et al., 2015; Niu et al., 2014; Shin et al., 2004a, b). The protein and gene expressions of iNOS, NF-*κ*B/p65 and COX-2 were detected in LPS-induced cells. According to western blot analysis (Fig. 9), LPS activation clearly increased the iNOS, NF-*κ*B/p65 and COX-2 protein levels when compared with controls in RAW 264.7 cells. However, compounds **3** and **4** remarkably inhibited LPS-induced iNOS, NF-*κ*B/p65 and COX-2 protein expressions in a concentration-dependent manner.

2.2.4. Structure – activity relationship analysis of the phenyl-naphthalene lignans from I. ternifolius

Bioassays verified that compounds **3** and **4** exhibited more potent inhibition of NO, PGE2 and TNF-*α* release than the positive control,

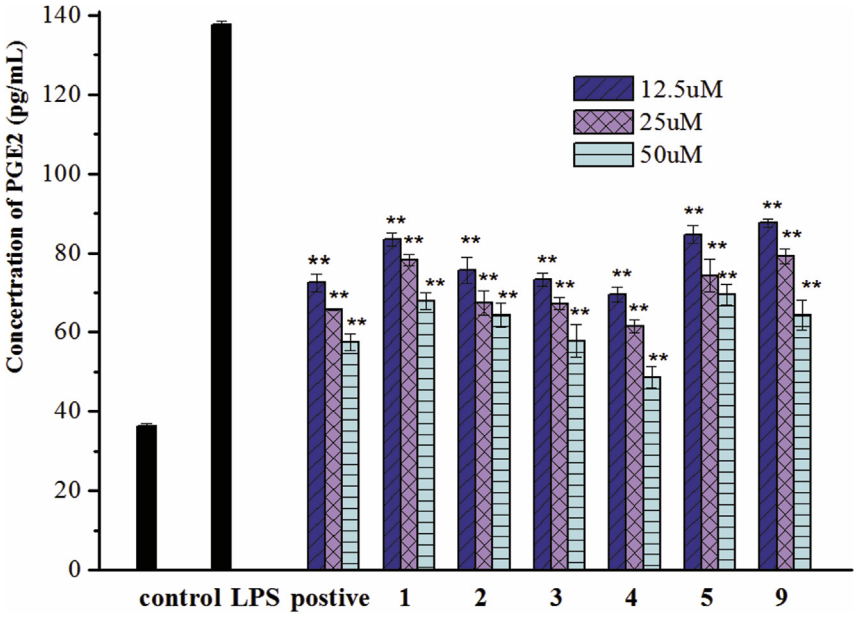

Fig. 8. Effects of the compounds **1**, **2**, **3**, **4**, 5 and **9** on the PGE2 production in LPS-stimulated RAW 264.7 cells. The cells were stimulated with LPS (100 ng/mL) 2 h and then for treated with the compounds (12.5, 25, 50 μM) for 24 h. PGE2 concentration in the supernatants was measured using ELISA. Indomethacin was used as positive reference compound at the same concentration with compounds. Values are the mean ± SE of three determinations. **p < 0.01 compared with cells treated by LPS.

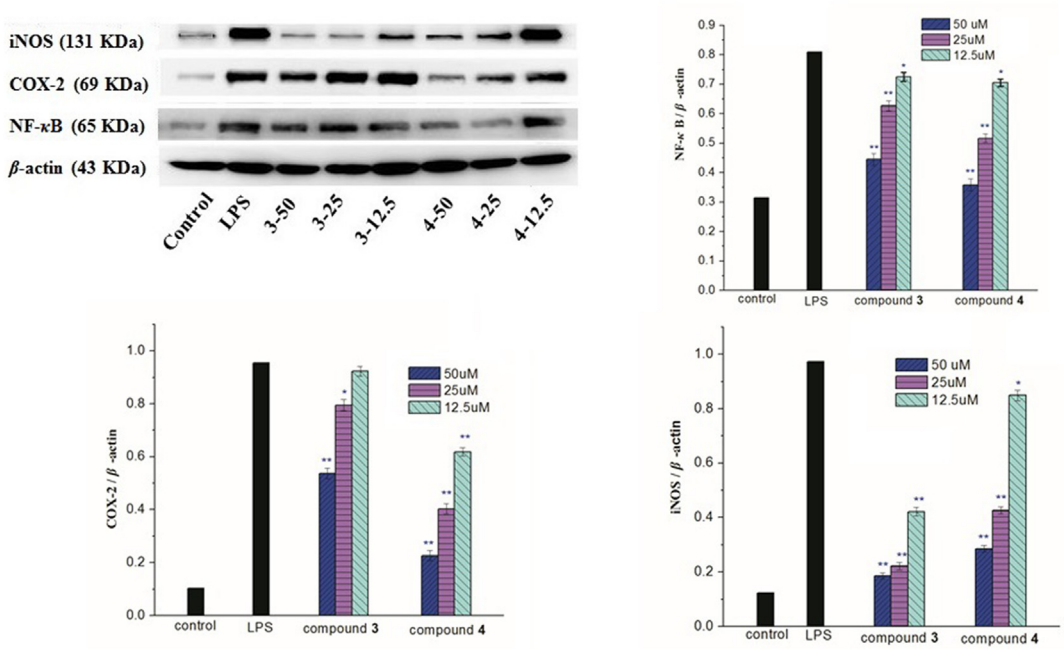

Fig. 9. Effects of compounds **3** and **4** at 12.5, 25, 50 μM concentrations on NF-κB/p65, COX-2. and iNOS expressions in LPS-induced RAW 264.7 cells, β-actin served as the loading control. **p < 0.01, *p < 0.05 compared with cells treated by LPS.

indomethacin. The lignans with phenyl-naphthalenes, such as compounds **3** and **4**, showed the strongest anti-inflammatory activities. Moreover, the anti-inflammatory activity of **4** is stronger than that of **3**, which indicated that the ester or carboxyl group linked to C-2 decreases the anti-inflammatory activity. A comparison of the anti-inflammatory activities of **4** and **9** suggested that the esterification of the C-9 carboxyl group could improve the anti-inflammatory activity. The anti-inflammatory activity of **1** is weaker than that of **2**, which indicates that the double bond between C-1 and C-2 could increase the anti-inflammatory activity. The anti-inflammatory activity of compound **3** is greater than that of **2**, suggesting that the esterification of C-9 is superior to the esterification of the C-10 carboxyl group.

3. Conclusions

In summary, five undescribed lignans, three undescribed phenylethanoid glycosides, and eight known compounds were isolated from *I. ternifolius*. Anti-inflammatory evaluation of the isolates suggested that some phenyl-naphthalene lignans have good anti-inflammatory activities; for example, compounds **3** and **4** could inhibit NO, TNF-α and PGE2 production as well as suppress the expressions of iNOS, NF-κB/p65 and COX-2 in LPS-induced RAW 264.7 cells. The anti- inflammatory activities of phenyl-naphthalene lignans were dependent on the structure, degree of hydrogenation of the naphthalene ring, substitution pattern of the carbonyl groups and esterification of the carbonyl groups. This report thus provides a basis for identifying the activity of this medicinal plant. These findings will enrich the chemotaxonomic diversity of the genus, which will aid in the pharmacological studies of natural products isolated from *I. ternifolius*.

4. Experimental

4.1. General

Optical rotations were measured on an Anton Paar MCP500 polarimeter (λ 589 nm, path length 1.0 cm). UV spectra were acquired with a TU-1901 spectrophotometer. CD spectra were recorded on a JASCO J-180 spectropolarimeter. IR spectra were measured with a Nicolet Avatar 360 FT-IR spectrometer. NMR experiments were conducted on Bruker Advance 500 MHz or 400 MHz spectrometers with residual solvent as the internal standard. HRESIMS were recorded on a Thermo MAT 95XP mass spectrometer. Semi-preparative HPLC separations were conducted on an Agilent 1260 instrument equipped with a DAD and an Agilent Zorbax SB-C_{18} column (5 μm, 9.4 × 250 mm) at a flow rate of 2.5 mL/min. Analytical HPLC was conducted on a Waters 2695 instrument equipped with a PAD detecter and a Waters C_{18} column (5 μm, 4.6 × 250 mm) at a flow rate of 1.0 mL/min. OD values of 96-well were measured with an imark Bio-Rad plate microplate reader. The expression levels of proteins were detected with an image station 4000R Pro luminescent image analyzer. Silica gel (200–300 mesh, Qingdao Marine Chemical Co. Ltd., China) and ODS C_{18} (50 μm, Merck, Germany) were used for the preliminary separation of crude samples, and a sephadex LH-20 column (Amersham Pharmacia Biotech AB, Sweden) as used for the final purification. D-glucose, L-glucose, D-rhamnose, and L-rhamnose were used as sugar standards (Sigma-Aldrich, Munich, Germany). Other chemicals were of analytical or HPLC grade.

4.2. Plant marterial

Dried root (22.0 kg) of *Isodon ternifolius* (D.Don) Kudô (Lamiaceae) was obtained from Jinxiu in Guangxi Province, China, in September a dry season, 2016 and identified by associate professor Yusong Huang (Guangxi Institute of Botany). A voucher specimen (No. ID-20160905) is deposited at the State Key Laboratory for the Chemistry and Molecular Engineering of Medicinal Resources, Guangxi Normal University, China.

4.3. Extraction and isolation

The dried powdered root of *I. ternifolius* (22.0 kg) was extracted with MeOH at room temperature (3 days × 3), and the combined extract was concentrated under reduced pressure. The dark brown extract (841.2 g) was suspended in H_2O and partitioned with EtOAc to give an EtOAc-soluble extract (353.0 g). The EtOAc extract was subjected to silica gel column chromatography and eluted with $CHCl_3$-EtOAc-MeOH mixtures

(1:0:0 to 0:1:1, v/v) to yield six fractions (Fr 1 to Fr 6). Fr 3 (23.5 g) was further purified on a silica gel column and eluted with mixtures of $CHCl_3$-EtOAc (1:0 to 0:1) to afford five fractions (Fr 3.1 to Fr 3.5). Compounds **11** (54.7 mg), **16** (5.5 mg) and **15** (10.6 mg) were obtained from Fr 3.1 (2.6 g) using Sephadex LH-20 CC (eluted with PE-CH_2Cl_2—MeOH 1:2:1). Fr 3.2 (15.2 g) was subjected to Sephadex LH-20 CC eluted with MeOH and semi-preparative HPLC (eluted with MeOH—H_2O, 45:55) to yield compound **4** (t_R 31.7 min, 7.0 mg). Fr 3.3 (4.2 g) was further purified on a C_{18} RP column and eluted with MeOH—H_2O (30:70, 45:55, 65:35, 80:20 and 100:0) to afford five subfractions (Fr 3.1.1 to Fr 3.1.5). Fr 3.3.2 was subjected to semi-preparative HPLC (eluted with MeOH—H_2O, 40:60) and Sephadex LH-20 CC (eluted with MeOH) to yield compound **13** (t_R 45.8 min, 7.3 mg). Fr 4 (44.0 g) was further fractionated on a silica gel column and eluted with mixtures of $CHCl_3$—MeOH (95:5 to 0:1) to afford six fractions (Fr 4.1 to Fr 4.6). Fr 4.2 (10.1 g) was further purified on a C_{18} RP silica gel column and eluted with MeOH—H_2O mixtures (9:1 to 1:0) to give five fractions (Fr 4.2.1 to Fr 4.2.5). Fr 4.2.2 was subjected to Sephadex LH-20 CC (eluted with MeOH) and semi-preparative HPLC (eluted with MeOH—H_2O, 53:47) to yield compounds **6** (t_R 21.5 min, 32.1 mg), **7** (t_R 35.5 min, 15.2 mg), and **8** (t_R 35.5 min, 13.6 mg). Fr 4.3 (18.1 g) was applied to a C_{18} RP silica gel column and eluted with MeOH—H_2O mixtures (9:1 to 1:0) to give five fractions (Fr 4.3.1 to Fr 4.3.5). Fr 4.3.2 (900.0 mg) was purified on a Sephadex LH-20 column eluted with MeOH to yield compounds **1** (23.2 mg), **10** (121.2 mg), and **3** (18.2 mg). Fr 4.3.3 (530.0 mg) was subjected to Sephadex LH-20 CC and eluted with MeOH to obtain compounds **2** (17.5 mg) and **9** (37.1 mg). Fr 4.3.4 (121.0 mg) was purified on a Sephadex LH-20 column and further purified by RP-HPLC eluted with MeOH—H_2O (60:40) to give compounds **12** (t_R 23.7 min, 54.0 mg) and **5** (t_R 33.5 min, 37.0 mg). Fr 4.6 (3.5 g) was subjected to semi-preparative HPLC (eluted with MeOH—H_2O, 10:90) to yield compound **14** (t_R 31.6 min, 4.1 mg).

4.4. Ternifoliuslignan A (1) [(1S,2R)-2,3-dicarboxy-6,7-dihydroxy-1-(3′,4′-dihydroxy)-phenyl-1,2 -dihydronaphthalen-10-ethyl ester]

Amorphous powder; $[\alpha]_D^{25}$ + 14.4 (*c* 0.20, MeOH); UV (MeOH) λ_{max} (log ε) 210 (4.28), 249 (2.73), 337 (1.80); IR (KBr) ν_{max} 3438, 3300, 2960, 1710, 1695, 1610, 1585, 1520, 1258, 1114 cm^{-1}; CD (MeOH) $\Delta\varepsilon$ 209 (+20.2), 240 (−17.2), 261 (+3.1), 343 (−3.7), 373 (+3.6), For ^1H NMR (CD_3OD, 400 MHz) and ^{13}C NMR (CD_3OD, 100 MHz) spectroscopic data, see Tables 1 and 2; HRESIMS *m/z* 409.0896 $[M + Na]^+$ (cald for $C_{20}H_{18}O_8Na$ 409.0899).

4.5. Ternifoliuslignan B (2) [2,3-dicarboxy-6,7-dihydroxy-1-(3′,4′-dihydroxy)-phenylnaphthalene-10 -ethyl ester

Amorphous powder; UV (MeOH) λ_{max} (log ε) 254 (2.51), 298 (3.56), 333 (3.28) nm; IR (KBr) ν_{max} 3440, 2980, 3300, 1707, 1690, 1625, 1594, 1530 cm^{-1}; For ^1H NMR (CD_3OD, 400 MHz) and ^{13}C NMR (CD_3OD, 100 MHz) spectroscopic data, see Tables 1 and 2; HRESIMS *m/z* 383.0754 $[M - H]^-$ (cald for $C_{20}H_{15}O_8$ 383.0767).

4.6. Ternifoliuslignan C (3) [2,3-dicarboxy-6,7-dihydroxy-1-(3′,4′-dihydroxy)-phenyl-naphthalene-9- ethyl ester]

Amorphous powder; UV (MeOH) λ_{max} (log ε) 254 (3.13), 295 (4.02), 334 (3.64) nm; IR (KBr) ν_{max} 3440, 2985, 1714, 1690, 1622, 1594, 1515 cm^{-1}; For ^1H NMR (CD_3OD, 400 MHz) and ^{13}C NMR (CD_3OD, 100 MHz) spectroscopic data, see Tables 1 and 2; HRESIMS *m/z* 407.0742 $[M + Na]^+$ (cald for $C_{20}H_{16}O_8Na$ 407.0743).

4.7. Ternifoliuslignan D (4) [3-carboxy-6,7-dihydroxy-1-(3′,4′-dihydroxy)-penylnaphthalene-9-ethyl ester]

Amorphous powder; UV (MeOH) λ_{max} (log ε) 255 (4.08), 303 (3.82) nm; IR (KBr) ν_{max} 3412, 2929, 1622, 1503, 1270, 1201 cm^{-1}; For ^1H NMR (CD_3OD, 400 MHz) and ^{13}C NMR (CD_3OD, 100 MHz) spectroscopic data, see Tables 1 and 2; HRESIMS *m/z* 363.0857 $[M + Na]^+$ (calcd for $C_{19}H_{16}O_6$ Na, 363.0845).

4.8. Ternifoliuslignan E (5) [2R-3-(3,4-dihydroxyphenyl)-2-[(3,4-dihdroxyphenyl)-6,7-dihydroxy -2- naphthoyloxy]-propanoic acid methyl ester]

Amorphous powder, $[\alpha]_D^{25}$ + 35 (c 0.15, MeOH); UV (MeOH) λ_{max} (log ε) 261 (4.35), 318 (1.12) nm; CD (MeOH) $\Delta\varepsilon$ 210 (+1.4), 228 (−3.2), 254 (+3.6); IR (KBr) ν_{max} 3415, 2930, 2854, 1697, 1602, 1523, 1452, 1385 cm^{-1}; For ^1H NMR (CD_3OD, 400 MHz) and ^{13}C NMR (CD_3OD, 100 MHz) spectroscopic data, see Tables 1 and 2; HRESIMS *m/z* 505.1118 $[M - H]^-$. (calcd for $C_{27}H_{21}O_{10}$, 505.1135).

4.9. Ternifoliusoside F (6) [1′-O-β-D-(3-hydroxy-4-methoxy-phenyl)-ethyl-4′-O-feruloyl-α-L-(4′′ -acetyl)-rhamnosyl(1′′→3′)-2′-acetyl-glucopyranoside]

Yellow gum; $[\alpha]_D^{25}$ − 15.7 (*c* 0.20, MeOH); UV (MeOH) λ_{max} (log ε) 210 (3.84), 330 (2.92) nm; IR (KBr) ν_{max} 3393, 2928, 1747, 1708, 1653, 1584, 1510, 809 cm^{-1}; For ^1H NMR (CD_3OD, 400 MHz) and ^{13}C NMR (CD_3OD, 100 MHz) spectroscopic data, see Table 3; HRESIMS *m/z* 759.2472 ($[M + Na]^+$, calcd for $C_{35}H_{44}O_{17}$ Na, 759.2476).

4.10. Ternifoliusoside G (7) [1′-O-β-D-(3-hydroxy-4-methoxy phenyl)-ethyl-6′-O-feruloyl-α-L-(4′′- acetyl)-rhamnosyl(1′′→3′)-2′-acetyl-glucopyranoside]

Yellow gum; $[\alpha]_D^{25}$ − 43.5 (*c* 0.20, MeOH); UV (MeOH) λ_{max} (log ε) 210 (4.08), 330 (3.07) nm; IR (KBr) ν_{max} 3392, 2930, 1747, 1708, 1652, 1594, 1515, 809 cm^{-1}; For ^1H NMR (CD_3OD, 400 MHz) and ^{13}C NMR (CD_3OD, 100 MHz) spectroscopic data, see Table 3; HRESIMS *m/z* 759.2469 ($[M + Na]^+$, calcd for $C_{35}H_{44}O_{17}Na$, 759.2476).

4.11. Ternifoliusoside H (8) [1′-O-β-D-(3-hydroxy-4-methoxyphenyl)-ethyl-6′-O-feruloyl-α-L- rhamnosyl(1′′→3′)-2′-acetyl-glucopyranoside]

Amorphous powder; $[\alpha]_D^{25}$ − 33.5 (*c* 0.21, MeOH); UV (MeOH) λ_{max} (log ε) 210 (4.15), 295 (3.28) nm; IR (KBr) ν_{max} 3364, 2930, 1747, 1708, 1652, 1594, 1515 cm^{-1}; For ^1H NMR (CD_3OD, 400 MHz) and ^{13}C NMR (CD_3OD, 100 MHz) spectroscopic data, see Table 3; HRESIMS *m/z* 717.2365 ($[M + Na]^+$, calcd for $C_{34}H_{42}O_{16}$ Na, 717.2370) (See supporting information).

4.12. Enzymatic hydrolysis of compounds 6–8

Acidic hydrolyses of compounds **6–8** were carried out according to the method described previously (Dai et al., 2017; He et al., 2017). The configurations of the sugar moieties were determined by comparing the R_f values of the products with the derivatives of authentic samples. The R_f values were 0.36 (D-glucose) and 0.65 (L-rhamnose). D-glucose and L-rhamnose were confirmed by comparison of their retention times and optical rotations with those of authentic samples; t_R (CH_3CN:H_2O, 78:22, v/v, 1 mL/min): 6.8 min (L-rhamnose, negative optical rotation) and 12.0 min (D-glucose, positive optical rotation).

4.13. Calculation of ECD spectra

The ECD spectra for the stable conformers were calculated by time-dependent (TD)-DFT at the B3LYP/6-311 + G (2d, p) level using the

polarizable continuum model in MeOH. The calculated ECD curves were generated using SpecDis 1.53 software (σ = 0.3 eV) (Bruhn et al., 2011). The final ECD spectra of (1R,2*S*)-**1** and (1*S*,2R)-**1** were obtained based on the Boltzmann-statistical contribution of each conformer and the experimental data. All DFT and TD-DFT calculations were conducted with Gaussian 09 program (Frisch et al., 2010).

4.14. Cell viability assay

The cell viabilities of the isolates and indomethacin (Sigma) as the positive control were determined using the MTT assay (Huang et al., 2016). The RAW 264.7 cells were plated in 96-well plates at 1×10^5 cell per well with 180 μL per well. After incubation overnight, the cells were stimulated with 10 μL of 2 μg/mL LPS for 2 h, treated with a series of diluted compounds or indomethacin (6.25, 12.5, 25, and 50 μM) at 10 μL for 24 h, and then cultured with 10 μL of MTT reagent for 4 h. The formazan crystals were dissolved with 100 μL of DMSO. The absorbance was measured at 570 nm with a microplate reader.

4.15. NO production assay

NO was detected by the Griess assay (Chen et al., 2017; Choi et al., 2012). The incubation procedure was the same as for the cell viability assay. After the cells had been treated with a series of compounds for 24 h, the production of NO in each supernatant was determined based on the Griess reaction, and the absorbance was measured at 550 nm in a microplate reader.

4.16. Enzyme-linked immunosorbent assay (ELISA)

The effects of phenyl-naphthalene lignans on cytokine (TNF-α and PGE2) release in RAW264.7 cells were evaluated using an ELISA. The RAW264.7 cells were seeded at a density of 3×10^4 cells per well in 96-well plates, and the compounds were added to cells after 2 h of LPS-stimulation. When RAW264.7 cells were treated with the compounds for 24 h, the TNF-α and PGE2 levels in cell culture supernatant were measured using an ELISA detection kit according to the manufacturer's instructions. Indomethacin was used as a positive control drug in this experiment.

4.17. Western blotting

RAW264.7 cells were seeded at a density of 2×10^6 cells per well in 6-well plates and was stimulated by LPS. And the compounds were added to cells after 2 h LPS-stimulation. When RAW264.7 cells were treated by the compounds for 24 h, the cells were collected for protein extraction and western-blot analysis. The cells were washed three times with ice-cold PBS. Cellular lysates were prepared in lysis buffer at 4 °C for 30 min and centrifuged at 12000 rpm. After the quantification of proteins by a bicinchoninic acid protein assay kit proteins, the protein was resolved by sodium dodecyl sulfate − polyacrylamide gel electrophoresis and transferred onto a polyvinylidene difluoride membrane. The membranes were treated with 10% skimmed milk in Tris-buffered saline containing 0.1% Tween 20 to block the nonspecific binding for 0.5 h at room temperature. After washing three times with TBST, the membranes were probed with anti-mouse iNOS antibody (dilution 1:1000), anti-mouse COX-2 antibody (dilution1:1000) or anti-mouse NF-κB/p65 antibody (dilution1:2000) overnight at 4 °C. Thereafter, the membranes were washed adequately with TBST and incubated with a horseradish peroxidase-conjugated secondary antibody at 37 °C for 2 h. The expression levels of iNOS, COX-2 and NF-κB/p65 proteins were observed on an image station 4000R Pro luminescent image analyzer. The density of the western blot bands was analysed using Quantity One software (Bio-Rad).

4.18. Statistical analysis

The data were presented as the mean ± standard deviation (SD) from at least three independent experiments. Statistical comparisons between groups were performed by Student's t-test. *p*-Value less than 0.05 was considered to be statistically significant.

Notes

The authors declare no competing financial interest.

Acknowledgements

One of the authors (J. L.) acknowledges the following grants for funding this project: National Natural Science Foundation of China (21662004); The Natural Science Foundation of Guangxi Province (2017GXNSFBA1980083); The Natural Science Foundation of Guangxi Province (2014GXNSFDA118008); The Open Research Fund program of the Key Laboratory for the Chemistry and Molecular Engineering of Medicinal Resources (CMEMR2012–A21).

Appendix A. Supplementary data

Supplementary data related to this article can be found at http://dx.doi.org/10.1016/j.phytochem.2018.05.017.

References

Bruhn, T., Hemberger, Y., Schaumlöffel, A., Bringmann, G., 2011. SpecDis: Version 1.53. University of Wuerzburg, Germany.
Chawla, A.S., Sharma, A.,K., Handa, S.S., Dhar, K.L., 1992. A lignan from *Vitex negundo* seeds. Phytochemistry 31, 4378–4379.
Chen, C.H., Hwang, T.L., Chen, L.C., Chang, T.H., Wei, C.S., Chen, J.J., 2017. Isoflavones and anti-inflammatory constituents from the fruits of *Psoralea corylifolia*. Phytochemistry 143, 186–193.
Chi, Q.Q., Wang, Q., Zhong, Y.Q., 2016. Advances on the research of the pharmacological activity mechanism and toxicology of glaucocalyxin A. J. Pharm. Pract. 34, 124–128.
Choi, W.S., Shin, P.G., Lee, J.H., Kim, G.D., 2012. The regulatory effect of veratric acid on NO production in LPS-stimulated RAW264.7 macrophage cells. Cell. Immunol. 280, 164–170.
Dai, L.M., Huang, R.Z., Zhang, B., Hua, J., Wang, H.S., Liang, D., 2017. Cytotoxic triterpenoid saponins from *Lysimachia foenum-graecum*. Phytochemistry 136, 165–174.
Delectis Florae reipublicae popularis sinicae agendae academiae sinicae edita, 1977. Flora republicae Popularis Sinicae, vol. 66. Science press, Beijing, pp. 416–532.
Deyama, T., Ikawa, T., Kitagawa, S., Nishibe, S., 1987. The constituents of *Eucommia ulmoides* Oliv. V. Isolation of dihydroxydehydrodiconiferyl alcohol isomers and phenolic compounds. Chem. Pharm. Bull. 35, 1785–1789.
Fedroreyev, S.A., Veselova, M.A., Krivoschekova, O.E., Mischenko, N.P., Denisenko, V.A., Dmitrenok, P.S., Glazunov, V.P., Bulgakov, V.P., Tchernoded, G.K., Zhuravlev, Y.N., 2005. Caffeic acid metabolites from *Eritrichium sericeum* cell cultures. Planta Med. 71, 446–451.
Frisch, M.J., Trucks, G.W., Schlegel, H.B., et al., 2010. Gaussian 09, Revision C. 01. Gaussian Inc., Wallingford, CT.
Guo, P., Li, Y.S., Guo, Y.Q., 2010. Advances in studies on chemical constituents of *Rabdosia rubescens* and their pharmacological activities. Drug Eval. Res. 33, 144–147.
He, R.J., Zhang, Y.J., Wu, L.D., Nie, H., Huang, Y., Liu, B.M., Deng, S.P., Yang, R.Y., Huang, S., Nong, Z.J., Li, J., Chen, H.Y., 2017. Benzofuran glycosides and coumarins from the bark of *Streblus indicus* (Bur.) Corner. Phytochemistry 138, 170–177.
Hong, S.S., Lee, S.A., Han, X.H., Jin, H.Z., Lee, J.H., Lee, D., Lee, J.J., Hong, J.T., Kim, Y., Ro, J.S., Hwang, B.Y., 2007. Kaurane diterpenoids from *Isodon excisus* inhibit LPS-induced NF- κB activation and NO production in macrophage RAW264.7 cells. J. Nat. Prod. 70, 632–636.
Huang, M.Y., Lin, J., Huang, Z.J., Xu, H.G., Hong, J., Sun, P.H., Guo, J.L., Chen, W.M., 2016. Design, synthesis and anti-inflammatory effects of novel 9-*O*-substituted-berberine derivatives. Med. Chem. Comm. 7, 658–666.
Jiang, B., Chen, X.R., Lu, Z.Q., Sun, H.D., 2000. A new lignan from *Isodon lophanthoides* var. gerardianus (Labiatae). Acta Bot. Sin. 42, 95–97.
Lee, C.H., Kim, J.H., Lee, H.J., Lee, S.M., Kho, Y.H., 2001. Two new constituents of *Isodon excisus* and their evaluation in an apoptosis inhibition assay. J. Nat. Prod. 64, 659–660.
Lee, J.W., Lee, M.S., Kim, T.H., Lee, H.J., Hong, S.S., Noh, Y.H., Hwang, B.Y., Ro, J.,S., Hong, J.T., 2007. Inhibitory effect of inflexinol on nitric oxide generation and iNOS expression via inhibition of NF-κB activation. Mediat. Inflamm. 4, 93148–93156.
Liu, M., Wang, W.G., Sun, H.D., Pu, J.X., 2017. Diterpenoids from *Isodon* species: an update. Nat. Prod. Rep. 34, 1090–1140.
Liu, Q., Hu, H.J., Li, P.F., Yang, Y.B., Wu, L.H., Chou, G.X., Wang, Z.T., 2014. Diterpenoids and phenylethanoid glycosides from the roots of *Clerodendrum bungei*

and their inhibitory effects against angiotensin converting enzyme and α-glucosidase. Phytochemistry 103, 196–202.
Ma, X.M., Liu, Y., Shi, Y.P., 2007. Phenolic derivatives with free-radical-scavenging activities from *Ixeridium gracile* (DC. Shhih. Chem. Biodivers. 4, 2172–2180.
Nishizawa, M., Tsuda, M., Hayashi, K., 1990. Two caffeic acid tetramers having enantiomeric phenyldihydronaphthalene moieties from *Macrotomia euchroma*. Phytochemistry 29, 2645–2649.
Niu, Y.G., Shang, P.P., Chen, L., Zhang, H., Gong, L., Zhang, X.W., Yu, W.J., Xu, Y.H., Wang, Q., Yu, L.L., 2014. Characterization of a novel alkali-soluble heteropolysaccharide from tetraploid *Gynostemma pentaphyllum* makino and its potential anti-inflammatory and antioxidant properties. J. Agric. Food Chem. 62, 3783–3790.
Ren, Y.M., Ke, C.Q., Mandi, A., Kurtan, T., Tang, C.P., Yao, S., Ye, Y., 2017. Two new lignan- iridoid glucoside diesters from the leaves of *Vaccinium bracteatum* and their relative and absolute configuration determination by DFT NMR and TDDFT -ECD calculation. Tetrahedron 73, 3213–3219.
Shin, K.M., Kim, I.T., Park, Y.M., Ha, J., Choi, J.W., Park, H.J., Lee, Y.S., Lee, K.T., 2004a. Anti-inflammatory effect of caffeic acid methyl ester and its mode of action through the inhibition of prostaglandin E2, nitric oxide and tumor necrosis factor-α production. Biochem. Pharmacol. 68, 2327–2336.
Shin, T.Y., Kim, S.H., Choi, C.H., Shin, H.Y., Kim, H.M., 2004b. *Isodon japonicus* decreases immediate-type allergic reaction and tumor necrosis factor-production. Int. Arch. Allergy Immunol. 135, 17–23.
Sun, J., Yu, J., Zhang, P.C., Yue, D.Y., 2015. Enantiomeric determination of four diastereoisomeric oxyneolignans from Bambusa tuldoides Munro. Phytochem. Anal. 26, 54–60.
Wang, Y., Li, C., Xiang, L., Huang, W., He, X., 2016. Spirostanol saponins from Chinese onion (*Allium chinense*) exert pronounced anti-inflammatory and antiproliferative activities. J. Funct. Foods 25, 208–219.
Wu, T.S., Yeh, J.H., Wu, P.L., 1995. The heartwood constituents of Tetradium glabrifolium. Phytochemistry 40, 121–124.
Wu, Z.Y., Li, X.W., 1977. Flora Repubulicae Popularis Sinicae, vol. 66. Science Press, Beijing, pp. 436–439.
Xie, C.F., Li, Z.J., Qu, J.J., Sun, B., Lou, H.X., 2007. Chemical constituents of two liverworts *dumortiera hirsute* and *Pallavicinia ambigua*. Chin. Pharmaceut. J. 42, 1706–1708.
Xu, J.F., Tan, N.H., Zhang, Y.M., Yang, Y.B., Bai, J.X., 2006. Chemical constituents from Sabina gaussenii. Chin. Tradit. Herb. Drugs 37, 838–876.
Yoshikawa, K., Mimura, N., Arihara, S., 1998. Isolation and absolute structures of enantiomeric 1,2-bis(4-hydroxy-3-methoxyphenyl)-1,3-propanediol 1-*O*-glucosides from the bark of *Hovenia trichocarpa*. J. Nat. Prod. 61, 1137–1139.
Yeom, M., Kim, J.H., Min, J.H., Hwang, M.K., Jung, H.S., Sohn, Y., 2015. Xanthii Fructus inhibits inflammatory responses in LPS stimulated RAW 264.7 macrophages through suppressing NF-κB and JNK/p38 MAPK. J. Ethnopharmacol. 176, 394–401.
Zou, J., Du, X., Pang, G., Shi, Y.M., Wang, W.G., Zhan, R., Kong, L.M., Li, X.N., Li, Y., Pu, J.X., Sun, H.D., 2012. Ternifolide A, a new diterpenoid possessing a rare macrolide motif from *Isodon ternifolius*. Org. Lett. 14, 3210–3213.